

# Acid-Responsive *N*-Heteroacene-Based Material Showing Multi-Emission Colors

Kyosuke Isoda<sup>\*[a]</sup>

An acid-responsive *N*-heteroacene-based material has been prepared, which shows a blue emission color in a film. The protonation of this material in a thin film gives rise to remarkable changes in luminescent color compared to that in solution states. As the protonation of *N*-heteroacene molecules in films gradually occurs, their emission color can be tuned by adjusting the exposure time of the thin films to HCl vapor.

Oligoacenes composed of a polycyclic aromatic hydrocarbon (PAH) framework are attractive as a representative candidate for the development of organic electronics.<sup>[1–3]</sup> Oligoacenes can show semiconducting and luminescent properties, which are applied for the fabrication of organic light-emitting diodes (OLEDs) and organic thin-film transistors (OFETs). The chemical modification of oligoacenes through the introduction of heteroatoms such as O, S, P, and N is one of the effective methods to tune the electronic and semiconducting properties for the exploration of novel functional  $\pi$ -conjugated frameworks.<sup>[4–10]</sup> Among them, the incorporation of imino-N atoms is advantageous, as a C=N bond can be substituted into the oligoacene framework with the preservation of Hückel aromaticity instead of a C=C bond, whereby these molecules are called *N*-heteroacenes.<sup>[9–14]</sup>

In general, oligoacenes, such as pentacene, function as electron-donor and *p*-type organic semiconductors, whereas *N*-heteroacenes serve as electron-acceptor and *n*-type semiconductors, and this difference is because of the substitution of electron-deficient imino-N atoms.<sup>[9–14]</sup> As *N*-heteroacenes can be prepared readily and are stable in air and light, these  $\pi$ -conjugated frameworks are expected to be suitable candidates for building blocks in the development of semiconducting materials in condensed states, such as crystalline and amorphous films. The groups of Bunz and Miao have reported the fabrication of *n*-type semiconductors in crystal states and the preparation of larger heteroacenes linearly substituted with triiso-

propyl (TISP) ethynyl groups.<sup>[15–19]</sup> Recently, some groups have reported a series of liquid-crystalline (LC) *N*-heteroacene derivatives self-organizing into ordered superstructures such as 1-dimensional (1D) columnar and 2-dimensional (2D) lamellar LC phases via non-covalent intermolecular interactions.<sup>[20–25]</sup> These thin films for lamellar LC structures can transport charge carriers such as electrons<sup>[21]</sup> and holes<sup>[24]</sup> through  $\pi$ - $\pi$  stacking between  $\pi$ -conjugated frameworks. Also, *N*-heteroacene derivatives have been applied for OLEDs and OFETs in condensed states.<sup>[18,19,26,27]</sup> On the other hand, in dilute solution states, *N*-heteroacene derivatives can show their intrinsic properties characteristic of imino-N atoms without specific intermolecular interactions between molecules.

A nitrogen atom a good recognition element, because lone-pair electrons with Lewis base character on an  $sp^2$ -hybridized orbital can interact with Lewis acids such as metal ions and protons. As these interactions should give rise to marked changes in UV/Vis absorption and luminescent spectra according to changes in the electronic properties of the molecules, *N*-heteroacenes are able to serve as ion-sensing moieties in solution states.<sup>[28–31]</sup> Also, it is known that the protonation of imino-N atoms enhances the electron-withdrawing ability of LUMO levels.<sup>[32]</sup> Herein, I present the design and synthesis of a photo-functional *N*-heteroacene derivative showing proton-responsive behavior in the condensed state. It is anticipated that the electronic properties of  $\pi$ -conjugated molecules in solid states are distinct from those in dilute solution states, because intermolecular interactions such as  $\pi$ - $\pi$  stacking should occur. Moreover, protonation of *N*-heteroacene derivatives in the condensed state is expected to bring about pronounced changes in electronic properties, providing a facile method for tuning of the optical and semiconducting properties. The developments of *N*-heteroacene-based proton-responsive materials in solution states has previously been achieved,<sup>[28–30]</sup> however, those in condensed states are limited.

Figure 1 shows the molecular design of a dibenzophenazine derivative based on *N*-heteroacenes. The dibenzophenazine framework, composed of 1,10-phenanthroline and quinoxaline moieties, is utilized as a building block for the fabrication of

[a] Dr. K. Isoda

Department of Advanced Materials Science  
Faculty of Engineering, Kagawa University  
2217-20 Hayashi-cho, Takamatsu  
Kagawa 761-0396 (Japan)  
E-mail: k-isoda@eng.kagawa-u.ac.jp

Supporting Information and the ORCID identification number for the author of this article can be found under <http://dx.doi.org/10.1002/open.201700007>.

© 2017 The Authors. Published by Wiley-VCH Verlag GmbH & Co. KGaA. This is an open access article under the terms of the Creative Commons Attribution-NonCommercial License, which permits use, distribution and reproduction in any medium, provided the original work is properly cited and is not used for commercial purposes.

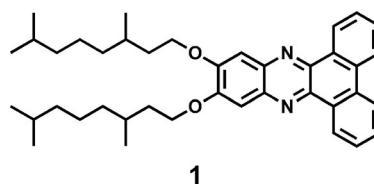


Figure 1. Molecular Structure of 1.

polymers<sup>[35]</sup> and discotic LC materials.<sup>[36–38]</sup> However, to the best of my knowledge, there is no report on the intrinsic electronic and stimuli-responsive properties of dibenzophenazine derivatives. The introduction of two long racemic alkoxy chains to the  $\pi$ -conjugated framework confers high solubility in various organic solvents, which can be easy to prepare as drop-cast films. The dibenzophenazine derivative was prepared according to previous procedures (see the Supporting Information).<sup>[20]</sup> Unfortunately, **1** exhibited no mesomorphism, as confirmed by polarized optical microscopic observations (see Figure S1). Cyclic voltammetry (CV) revealed that **1** shows a single reversible reduction wave at the half-wave potential  $E_1$  of  $-1.82$  V versus  $\text{Ag}/\text{Ag}^+$ , as derived from the formation of radical anion of **1** (see Figure S2), suggesting that **1** should function as an electron acceptor. It is noted that the addition of an excess of HCl gave rise to a remarkable change in the CV spectrum compared to **1** without HCl (see Figure S3). Two reversible redox peaks at  $E_1 = -0.28$  and  $E_2 = -0.59$  V for protonated **1** appear to be accompanied by the disappearance of **1**, indicating an increase in an electron-acceptor property of **1**. Akutagawa and Saito have also reported that the protonation of bimidazole containing imino-N atoms enhances the electron-acceptor property.<sup>[37]</sup> These results indicate that protonation is an effective method to modify the electronic properties of **1**.

The UV/Vis absorption and fluorescent spectra of **1** in solution states were measured to investigate the electronic properties in the ground and excited states, respectively, as shown in Figure 2. The UV/Vis absorption spectrum of **1** ( $10^{-6}$  M) shows two absorption peaks at 389 and 409 nm, and these peaks

remain very similar at various concentrations (from  $10^{-5}$  to  $10^{-3}$  M), as shown in Figure 2a. This result indicates that specific molecular associations do not occur in the ground state in solutions at these concentrations. On the other hand, increasing the concentration of **1** in solution leads to clear changes in the fluorescence spectra under excitation at 390 nm, as shown in Figure 2b. At a lower concentration ( $10^{-6}$  M), the fluorescence spectrum showed a peak at 422 nm with a broad shoulder around 440 nm. As the concentration of **1** in solution was increased from  $10^{-6}$  to  $10^{-3}$  M, the emission intensity at 440 nm was increased, accompanied by a decrease in that at 422 nm. The concentration dependence of **1** in solution was observed in fluorescence spectra because of the occurrence of an excited state, but it was not observed in UV/Vis spectra, owing to a ground state. The excitation spectra at higher concentrations ( $10^{-3}$  and  $10^{-4}$  M) were also different from those at lower concentrations ( $10^{-5}$  and  $10^{-6}$  M), indicating the formation of different excited states between at lower and higher concentrations (see Figure S4). These results suggest that emission peaks at around 420 and 440 nm can be ascribed to the monomer and to excimer formation, respectively.

When an excess of HCl was added into solutions of **1**, an obvious red shift of the lowest energy absorption peak from 440 to 467 nm was observed in the UV/Vis spectrum at  $10^{-6}$  M, as shown in Figure 2a. This indicated a change in the electronic properties of **1**, owing to an interaction between protons and imino-N atoms within **1**. Also, changes in the UV/Vis absorption spectra of protonated **1** in solution were not observed with increasing concentrations, as the behavior remained similar to that without a protonation of **1** in the ground state. In contrast, the fluorescent spectra of **1** show pronounced changes with increasing concentrations of **1** in solution, as shown in Figure 2b. Upon excitation at 460 nm, corresponding to the peak generated by protonated **1**, a new peak at 490 nm appeared at a lower concentration ( $10^{-6}$  M). As this peak was gradually red-shifted with increasing concentration of **1**, the emission spectrum for  $10^{-3}$  M shows the peak at 513 nm. The excitation spectra of **1** at  $10^{-3}$  M and  $10^{-6}$  M were measured to investigate the emission properties of peaks that appeared around 500 nm (see Figure S5). It is noted that the excitation spectrum obtained at  $10^{-3}$  M is different to that at  $10^{-6}$  M. In particular, the excitation spectrum obtained for  $10^{-3}$  M showed the new peak at 360 nm. Also, excitation at 360 nm gives rise to the pronounced enhancement of a peak intensity around 510 nm, which becomes 6.7 times larger than that observed upon excitation at 460 nm (see Figure S6). As a result, the emission species at  $10^{-3}$  M must be different to the monomer at  $10^{-6}$  M in the dilute state, which is derived from an excimer with a weak emission intensity. Also, the decrease in the emission intensity of **1** at  $10^{-3}$  M is considered to be characteristic of self-quenching, owing to the high concentration. Next, the protonation of drop-cast films in a condensed state upon exposure to HCl vapor is demonstrated in comparison to that in the solution state.

The UV/Vis absorption spectrum of a drop-cast film of **1** shows two peaks at 390 and 411 nm, which are similar to those in a dilute solution state, as shown in Figure 3a. This

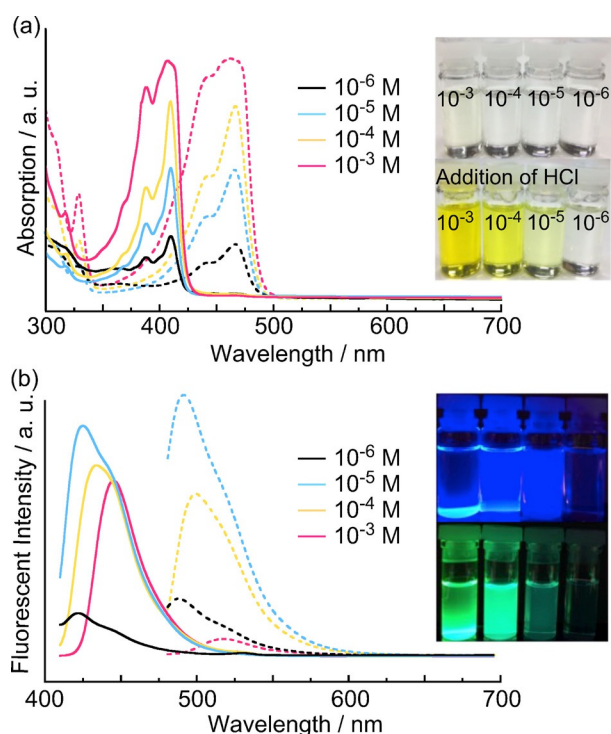


**Figure 2.** a) UV/Vis absorption and b) fluorescence spectra (excited at 390 nm) of **1** in  $\text{CHCl}_3$  solution without (solid line) and with (dashed line) excess HCl. Photographs show the  $\text{CHCl}_3$  solution of **1** with and without HCl under room light (top) and 365 nm light (bottom).

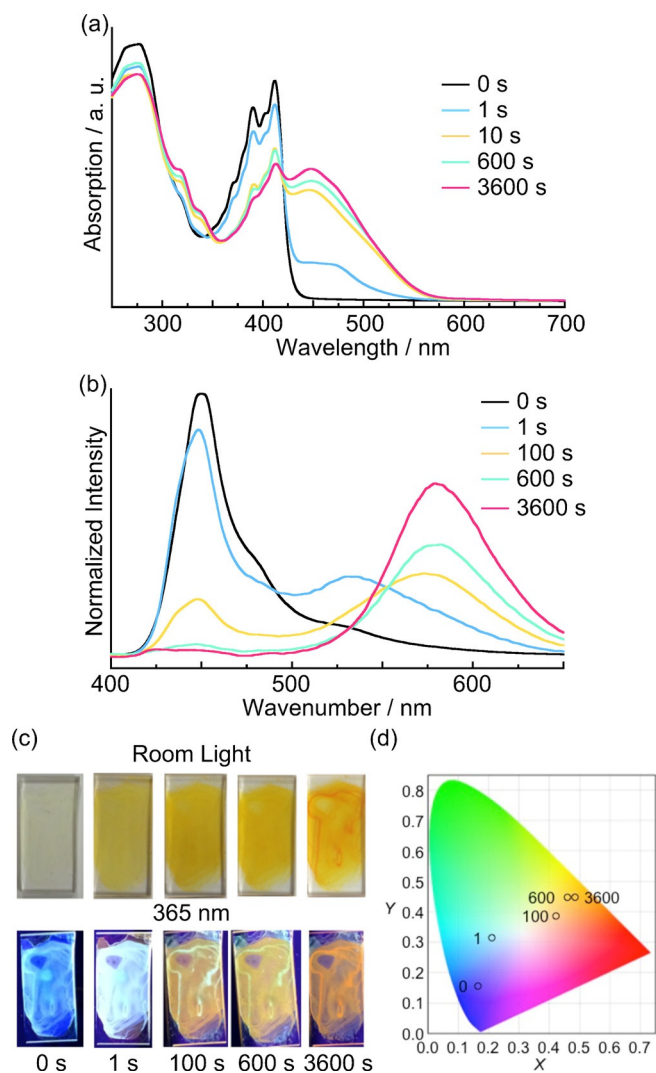


**Figure 3.** Time-dependent a) UV/Vis absorption and b) fluorescence spectra (excited at 390 nm) of films of **1** with exposure to HCl vapor. c) Photographs show time-dependence of films of **1** treated with HCl under room light (top) and 365 nm light (bottom). d) Plots of the Commission Internationale de l'éclairage (CIE) 1931 chromaticity diagram for time-dependent emission colors of films of **1** after treatment with HCl vapor.

suggests that specific intermolecular interactions scarcely occur between  $\pi$ -conjugated frameworks within films. When drop-cast films of **1** were exposed to HCl vapor, the absorption intensity at 449 nm gradually increased with exposure time, and was accompanied by a decrease in those at 390 and 411 nm. The intensity ratio at 449 nm relative to at 411 nm became larger with prolonged exposure to HCl vapor. It is noted that the lowest absorption edge in films treated with HCl vapor was clearly red-shifted compared to those in solutions, supporting that notion that intermolecular  $\pi$ - $\pi$  interactions<sup>[38]</sup> are induced by the protonation in a condensed state. For the fluorescence spectra of drop-cast films, dramatic changes were observed upon exposure to HCl vapor compared to those in dilute solution states.

Treatment with HCl vapor for films of **1** gave rise to an appearance of a new broad peak at around 580 nm, together

with a marked decrease in the peak intensity at 450 nm. The peak observed at 580 nm in a condensed state is more bathochromically shifted than that around at 500 nm in dilute solution states. This suggests that the protonation of **1** in a condensed state should enhance the emission characteristics of molecular aggregation. Also, it was found that the protonation of *N*-heteroacene molecules in films should gradually occur. As the degree of protonation can be adjusted in films by varying the time exposed to HCl vapor, luminescent film colors can be easily tuned under excitation at 390 nm. Figures 3c and 3d show that the emission colors of films are markedly changed from blue (0 s), to light blue (1 s), to light yellow (100 s), and to orange (600 s). The protonation of nonionic **1** should induce *N*-heteroacene ionic properties within the framework. Protonated **1** became an amphiphilic molecule composed of an ionic  $\pi$ -conjugated framework and hydrophobic long alkoxy chains, leading to an enhancement of molecular aggregation through nano-segregation<sup>[39]</sup> and a fastener effect<sup>[40]</sup> between the  $\pi$ -conjugated framework and the alkoxy chains. Moreover, the clearing temperature of protonated **1** (110 °C) is higher than that of **1** (92 °C), which is indicative of the enhancement of intermolecular interactions. As a result, protonation in the condensed state should enhance electronic changes of *N*-heteroacene derivatives, leading to larger bathochromic shifts than that of solution states. Then, X-ray diffraction (XRD) measurements were performed to investigate whether exposure to HCl vapor affects molecular arrangements in drop-cast films of **1** at room temperature.

The XRD pattern of **1** at room temperature shows an intense reflection peak at 23.9 Å with three small peaks at 12.1, 8.1, and 6.1 Å with reciprocal *d*-spacing ratios of 1:2:3:4, as shown in Figure 4. These peaks can be assigned as the Miller indices of (001), (002), (003), and (004), respectively, indicating that the molecules would be arranged to form a lamellar structure in a drop-cast film (see Figure S5 and Table S1). Although the molecular length of **1** is estimated to be approximately 21 Å, the *d* spacing of 23.9 Å obtained from the XRD pattern of the lamellar structure is longer than the molecular distance (see Figure S8). Dibenzophenazine frameworks of **1** adapt the *anti*-par-

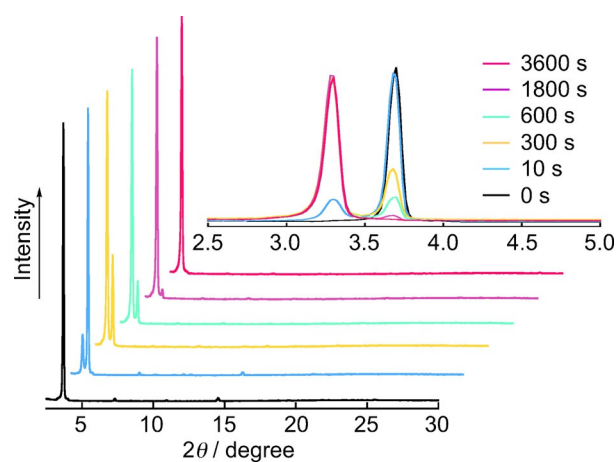


**Figure 4.** Time-dependent XRD patterns of films of **1** with exposure to HCl vapor. The inset shows the magnified views in the small-angle region.

allel manner<sup>[35]</sup> and the long alkoxy chains are partially interdigitated in the bilayer lamellar structure. The peak intensity caused by the  $d_{001}$  spacing became smaller with prolonged exposure of films of **1** to HCl vapor. Alternatively, the new peak at 26.9 Å in a smaller angle region gradually appeared (Figure 4, inset), suggesting that the protonation on *N*-heteroacene molecules occurs gradually, which should correspond to the results of spectral measurements. Similarly, shifts of the other three peaks to the smaller angle region were also observed (see Figure S5 and Table S1). These *d*-spacing values with reciprocal ratios of 1:2:3:4, calculated from the shifted peaks, are also indicative of the formation of a lamellar structure. As a result, the protonation of molecules in films should induce a rearrangement of molecular assembly to enhance intermolecular interactions. The induced molecular aggregates should markedly change the fluorescence spectra in comparison with those in dilute solution states.

Finally, I investigated the reversibility between protonation and deprotonation by using <sup>1</sup>H NMR and XRD measurements. The <sup>1</sup>H NMR spectrum in CDCl<sub>3</sub> solution, prepared from the film of **1** exposed to HCl vapor for 1 h, was much different to the spectrum for **1** itself (see Figure S9). The clear downfield shift of these peaks derived from H<sub>a</sub> and H<sub>b</sub> near to the imino-N atoms was observed as well as the appearance of a new broad peak at 8.5 ppm. These results suggest that protonation happens on two imino-N atoms even in films in a condensed state. Then, upon heating the film treated with HCl vapor under vacuum for 1 h, the <sup>1</sup>H NMR spectrum was recovered to that of the initial state before treatment with HCl vapor. This reversible behavior was also confirmed from results of XRD measurements in the films (see Figure S10). Moreover, the UV/Vis absorption spectrum of the film treated with HCl vapor can be almost recovered to that before protonation by exposure to NH<sub>3</sub> vapor at room temperature and ambient pressure (see Figure S11).

In summary, I have designed and synthesized a proton-responsive *N*-heteroacene-based material that exhibits luminescent properties in films. This material can be protonated by exposure to HCl vapor, resulting in remarkable changes in the emission colors. The protonation of *N*-heteroacene molecules in films influences the electronic properties of molecules and induces a rearrangement of the molecular assembly to enhance intermolecular interactions. The emission colors of their films can be readily tuned by adjusting exposure times to HCl vapor. Also, the reversible reactions of films between protonation and deprotonation are achieved by heating and exposure to NH<sub>3</sub> vapor. Recently, metal-organic frameworks (MOFs) have been widely investigated as representative materials for gas absorption.<sup>[41]</sup> However, absorption tests using MOFs have been operated under high pressure and low temperature. Treatment with acid gases tends to collapse the coordination bonding formed in MOFs. As this *N*-heteroacene-based material can absorb HCl vapor under ambient conditions, it is expected to offer a novel class of acid-sensing materials.

## Acknowledgements

This work was supported by a Grant-in-Aid for Scientific Research on Innovative Areas of "New Polymeric Materials Based on Element-Blocks (No. 2401)" (JSPS KAKENHI grant number JP25102540, JP15H00764) and for Scientific Research (C) (JSPS KAKENHI grant number 26410099) from the Ministry of Education, Culture, Sports, Science, and Technology of Japan, Shorai Foundation For Science and Technology, The Murata Science Foundation, and Young Scientists Fund for 2016 of Kagawa University Research Promotion Program (KURPP). I thank Dr. A. Sonoda at Health Research Institute, National Institute of Advanced Industrial Science and Technology for help with the NMR measurements.

## Conflict of Interest

The authors declare no conflict of interest.

**Keywords:** fluorescence • *N*-heteroacene • self-assembly • stimuli response •  $\pi$ -conjugated frameworks

- [1] J. E. Anthony, *Angew. Chem. Int. Ed.* **2008**, *47*, 452; *Angew. Chem.* **2008**, *120*, 460.
- [2] J. E. Anthony, *Chem. Rev.* **2006**, *106*, 5028.
- [3] A. R. Murphy, J. M. J. Fréchet, *Chem. Rev.* **2007**, *107*, 1066.
- [4] X.-Y. Wang, J.-Y. Wang, J. Pei, *Chem. Eur. J.* **2015**, *21*, 3528.
- [5] W. Jiang, Y. Li, Z. Wang, *Chem. Soc. Rev.* **2013**, *42*, 6113.
- [6] M. Stolar, T. Baumgartner, *Chem. Asian J.* **2014**, *9*, 1212.
- [7] T. Baumgartner, R. Réau, *Chem. Rev.* **2006**, *106*, 4681.
- [8] J. Li, Q. Zhang, *ACS Appl. Mater. Interfaces* **2015**, *7*, 28049.
- [9] U. H. F. Bunz, *Chem. Eur. J.* **2009**, *15*, 6780.
- [10] U. H. F. Bunz, J. U. Engelhart, B. D. Lindner, M. Schaffroth, *Angew. Chem. Int. Ed.* **2013**, *52*, 3810; *Angew. Chem.* **2013**, *125*, 3898.
- [11] U. H. F. Bunz, *Acc. Chem. Res.* **2015**, *48*, 1676.
- [12] Q. Miao, *Adv. Mater.* **2014**, *26*, 5541.
- [13] K. Isoda, M. Nakamura, T. Tatenuma, H. Ogata, T. Sugaya, M. Tadokoro, *Chem. Lett.* **2012**, *41*, 937.
- [14] G. J. Richards, J. P. Hill, N. K. Subbaiyan, F. D'Souza, P. A. Karr, M. R. J. Elsegood, S. J. Teat, T. Mori, K. Ariga, *J. Org. Chem.* **2009**, *74*, 8914.
- [15] F. Geyer, S. Schmid, V. Brosius, M. Bojanowski, G. Bollmann, K. Broedner, U. H. F. Bunz, *Chem. Commun.* **2016**, *52*, 5702.
- [16] F. Paulus, J. Engelhart, P. Hopkinson, C. Schimpf, A. Leineweber, H. Sirringhaus, Y. Vaynzof, U. H. F. Bunz, *J. Mater. Chem. C* **2016**, *4*, 1194.
- [17] U. H. F. Bunz, J. U. Engelhart, *Chem. Eur. J.* **2016**, *22*, 4680.
- [18] Z. Liang, Q. Tang, J. Xu, Q. Miao, *Adv. Mater.* **2011**, *23*, 1535.
- [19] Z. Liang, Q. Tian, R. Mao, D. Liu, J. Xu, Q. Miao, *Adv. Mater.* **2011**, *23*, 5514.
- [20] K. Isoda, T. Abe, M. Tadokoro, *Chem. Asian J.* **2013**, *8*, 2951.
- [21] K. Isoda, T. Abe, M. Funahashi, M. Tadokoro, *Chem. Eur. J.* **2014**, *20*, 7232.
- [22] K. Isoda, T. Abe, I. Kawamoto, M. Tadokoro, *Chem. Lett.* **2014**, *44*, 126.
- [23] T. Abe, M. Matsuzaka, K. Isoda, M. Tadokoro, *Mol. Cryst. Liq. Cryst.* **2015**, *615*, 70.
- [24] T. Takeda, J. Tsutsumi, T. Hasegawa, S. Noro, T. Nakamura, T. Akutagawa, *J. Mater. Chem. C* **2015**, *3*, 3016.
- [25] K. Isoda, I. Kawamoto, A. Seki, M. Funahashi, M. Tadokoro, *ChemistrySelect*, **2017**, *2*, 300.
- [26] B. D. Lindner, Y. Zhang, S. Höfle, N. Berger, C. Teusch, M. Jesper, K. I. Hardcastle, X. Qian, U. Lemmer, A. Colsmann, U. H. F. Bunz, *J. Hamburger, J. Mater. Chem. C* **2013**, *1*, 5718.
- [27] P. Biegger, S. Sebastian, S. N. Intorp, Z. Yexiang, J. U. Engelhart, F. Rominger, K. I. Hardcastle, U. Lemmer, X. Qian, M. Hamburger, U. H. F. Bunz, *J. Org. Chem.* **2015**, *80*, 582.

- [28] S. Kothavale, N. Sekar, *Dyes Pigm.* **2017**, *136*, 31.
- [29] P. Singh, A. Baheti, K. R. J. Thomas, *J. Org. Chem.* **2011**, *76*, 6134.
- [30] G. Li, A. P. Abiyasa, J. Gao, Y. Divayana, W. Chen, Y. Zhao, X. W. Sun, Q. Zhang, *Asian J. Org. Chem.* **2012**, *1*, 346.
- [31] Z. Yang, W. Qin, J. W. Y. Lam, S. Chen, H. H. Y. Sung, I. D. Williams, B. Z. Tang, *Chem. Sci.* **2013**, *4*, 3725.
- [32] Y. Dong, J. Zhang, X. Tan, L. Wang, J. Chen, B. Li, L. Ye, B. Xu, B. Zou, W. Tian, *J. Mater. Chem. C*, **2013**, *1*, 7554.
- [33] Y. Zhu, K. M. Gibbons, A. P. Kulkarni, S. A. Jenekhe, *Macromolecules* **2007**, *40*, 804.
- [34] E. J. Foster, C. Lavigueur, Y.-C. Ke, V. E. Williams, *J. Mater. Chem.* **2005**, *15*, 4062.
- [35] E. J. Foster, R. B. Jones, C. Lavigueur, V. E. Williams, *J. Am. Chem. Soc.* **2006**, *128*, 8569.
- [36] M.-C. Yeh, Y.-L. Su, M.-C. Tzeng, C. W. Ong, T. Kajitani, H. Enozawa, M. Takata, Y. Koizumi, A. Saeki, S. Seki, T. Fukushima, *Angew. Chem. Int. Ed.* **2013**, *52*, 1031; *Angew. Chem.* **2013**, *125*, 1065.
- [37] T. Akutagawa, G. Saito, *Bull. Chem. Soc. Jpn.* **1995**, *68*, 1753.
- [38] K. K. McGrath, K. Jang, K. A. Robins, D.-C. Lee, *Chem. Eur. J.* **2009**, *15*, 4070.
- [39] T. Kato, N. Mizoshita, K. Kishimoto, *Angew. Chem. Int. Ed.* **2006**, *45*, 38; *Angew. Chem.* **2006**, *118*, 44.
- [40] K. Ohta, M. Ikejima, M. Moriya, H. Hasebe, I. Yamamoto, *J. Mater. Chem.* **1998**, *8*, 1971.
- [41] S. Kitagawa, R. Kitaura, S. Noro, *Angew. Chem. Int. Ed.* **2004**, *43*, 2334; *Angew. Chem.* **2004**, *116*, 2388.

---

 Received: January 13, 2017

Revised: February 2, 2017

Published online on February 22, 2017